Equilibrium and Kinetic Parameters for the Binding of Inhibitors to the Q_B Pocket in Bacterial Chromatophores: Dependence on the State of Q_A[†]

Nicolas Ginet and Jérôme Lavergne*

CEA-Cadarache, DSV-DEVM, Laboratoire de Bioénergétique Cellulaire, 13108 Saint-Paul-lez-Durance, France

Received July 19, 2000; Revised Manuscript Received November 9, 2000

ABSTRACT: The equilibrium and kinetic parameters for the binding of various inhibitors to the Q_B pocket of the bacterial reaction center were investigated in chromatophores from *Rhodobacter capsulatus* and *Rhodobacter sphaeroides*. By monitoring the near-IR absorption changes specific to Q_A^- and Q_B^-, we measured the fraction of inhibited centers in the dark and the kinetics and extent of inhibitor displacement after one flash due to the formation of the $Q_AQ_B^-$ state. The inhibitor release rate was much faster for triazines and *o*-phenanthroline ($t_{1/2}$ in the 50 ms to 1 s range) than for stigmatellin ($t_{1/2} \approx 20$ s). For inhibitors with a rapid release rate, the fast phase of P^+ decay observed in the absence of secondary donor reflects the competition between $P^+Q_A^-$ recombination and inhibitor release: it is thus faster than the $P^+Q_A^-$ recombination, and its relative extent is smaller than the fraction of initially inhibited centers. At appropriate inhibitor concentrations, one can have almost total binding in the dark and almost total inhibitor displacement after one flash. Under such conditions, a pair of closely spaced flashes resets the two-electron gate in a single state ($Q_AQ_B^-$), irrespective of the initial state. The apparent dissociation constant of terbutryn was significantly increased (by a factor of 4−7) in the presence of Q_A^-, in agreement with the conclusion of Wraight and co-workers [Stein, R. R., et al. (1984) *J. Cell. Biochem*. *24*, 243−259]. We suggest that this effect is essentially due to a tighter binding of ubiquinone in the Q_A^- state.

The photosynthetic reaction centers of bacteria or of photosystem II in chloroplasts promote the reduction of a lipid-soluble pool of quinone molecules (ubiquinone-10 in bacteria or plastoquinone-9 in chloroplasts). This process involves two quinone cofactors in the reaction center complex. A primary quinone acceptor, denoted Q_A,[1] is tightly bound to the protein. It undergoes a fast reduction (∼200 ps) following the photochemical charge separation and then transfers its electron to a secondary quinone Q_B. Whereas Q_A shuttles between two redox states (oxidized quinone and singly reduced semiquinone), Q_B goes through a cycle involving three states (quinone, semiquinone, and the doubly reduced and protonated quinol). The fully oxidized and fully reduced forms are weakly bound to the RC complex at a special site (the Q_B pocket) and are rapidly exchanged with molecules of the pool. The semiquinone form, however, is strongly attached to the Q_B pocket (*1*). The positions and H-bond links of the quinone in its oxidized or semiquinone forms have been recently described from crystallographic investigations in bacterial RCs (*5*, *6*). The overall cycle of the "two-electron gate" is summarized by the following reactions:

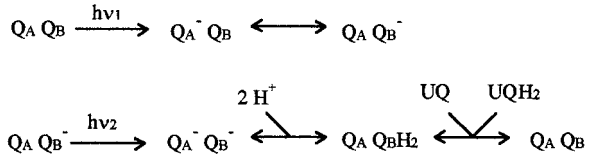

where $h\nu_1$ and $h\nu_2$ denote two successive photoacts, Q_A^- and Q_B^- are semiquinone states, and Q_BH_2 denotes the bound quinol before it is released from the Q_B pocket and replaced with a fresh quinone (UQ) from the pool. The protonation steps involved in the formation of quinol have been the focus of a number of recent studies (see ref *7* for a review).

A number of inhibitors are able to block the electron transfer from Q_A to Q_B. Many of them are effective in both bacterial RCs and PS II, and some of the PS II inhibitors are widely used as herbicides. It was shown in papers dating back to the 1980s that they act as competitors for quinone binding to the Q_B pocket (*4*, *8*−*11*). Due to the tight binding of the semiquinone form Q_B^-, the dissociation constant of the inhibitor is larger in the "odd" state of the quinone acceptor system (i.e., $Q_A^-Q_B \leftrightarrow Q_AQ_B^-$) than in the "even" state ($Q_AQ_BH_2 \leftrightarrow Q_AQ_B$) (this nomenclature, referring to the number of electrons present on the RC acceptor side, was introduced in ref *12*). In other words, if we note Q_AI the RC with bound inibitor, the light-induced formation of Q_A^-I will tend to displace the inhibitor according to the equilibrium $Q_A^-I + UQ \leftrightarrow Q_AQ_B^- + I$. Early evidence for this effect was reported by Verméglio et al. (*13*) before the elaboration of the Q_B pocket concept. A mathematical analysis of the equilibria and kinetics discussed in this paper is given in the Appendix, where symbol definitions and all numbered equations mentioned in the following are located.

In this paper, we analyze the kinetics of the inhibitor displacement in bacterial RCs by directly monitoring the decrease in the level of Q_A^- and formation of Q_B^-. The rate constants for inhibitor binding and release are thus deter-

[†] This work was supported by the CEA and CNRS.

* To whom correspondence should be addressed. Telephone: (33) 4 42 25 45 80. Fax: (33) 4 42 25 47 01. E-mail: jerome.lavergne@cea.fr.

[1] Abbreviations: BPhe, bacteriopheophytin; *o*-phe (or *o*-phenanthroline), 1,10-phenanthroline; Q_A, primary quinone acceptor; Q_B, secondary quinone acceptor; RC, reaction center; stig, stigmatellin; TMPD, *N*,*N*,*N*′,*N*′-tetramethyl-1,4-phenylenediamine; UQ, ubiquinone-10.

10.1021/bi001686a CCC: $20.00
Published on Web 01/18/2001

mined. An experimentally useful consequence of the displacement process will be described, allowing the light-induced "resetting" of the two-electron gate cycle. Our data also allow us to measure the inhibitor's dissociation constants in the even or odd state of the RC, confirming the finding of Wraight and co-workers (*4*) of a weaker binding in the presence of Q_A^-.

MATERIALS AND METHODS

The mutant FJ2 of *Rhodobacter capsulatus* was a kind gift of F. Daldal (*14*). It is devoid of the physiological donors to the RC (cytochromes c_2 and c_y). A similar strain for *Rhodobacter sphaeroides*, CYC17, was a kind gift of T. J. Donohue (*15*). This mutant lacks cytochrome c_2 and iso-c_2. Growth conditions and chromatophore preparation were previously described (*16*).

For spectroscopic experiments, the chromatophores were diluted in a medium containing 50 mM KCl and 50 mM Tris or MOPS buffer (pH 7.2). The RC concentration of the chromatophore suspension was ~100 nM, based on an extinction coefficient of 20 mM^{-1} cm^{-1} for P^+ at 600 nm. Valinomycin (3 μM) was generally added to collapse the membrane potential and associated absorption changes. In experiments using the exogenous donor TMPD (1 mM), the suspension was kept anaerobic under an argon flow and (when indicated) 5 mM KCN was added for suppressing the oxidase-mediated autoxidation of TMPD.

The inhibitors that were used were stigmatellin (Fluka), terbutryn (Chem Service), atrazine (Supelco), and *o*-phenanthroline (Sigma).

Absorption changes were assessed using a Joliot-type spectrophotometer (*17*, *18*), as previously described (*16*).

RESULTS

Figure 1 (top) shows the effect in chromatophores of the *R. capsulatus* mutant FJ2 of a range of terbutryn concentrations on the kinetics of P^+ reduction following a short saturating flash. Due to the absence of an electron donor to P^+ in this material, the control kinetics (no inhibitor) are due to the recombination reaction $P^+Q_B^- \rightarrow PQ_B$, with a $t_{1/2}$ of ≈3.5 s at pH 7.2. In the presence of inhibitor, a fast phase appears in the tens of milliseconds, reflecting the recombination $P^+Q_A^- \rightarrow PQ_A$ in inhibited centers. When the inhibitor concentration is increased, the extent of the fast phase increases, but this effect tends to level off so that at the highest concentration that was used, the relative amplitude of the slow phase is still about 50%. Atrazine, belonging to the same class of triazine inhibitors as terbutryn, gave similar results (not shown), although its effect on the slow phase was more pronounced (~15% at 100 μM). The bottom panel of Figure 1 shows the results from a similar experiment using the inhibitor stigmatellin. The latter is much more efficient in suppressing the slow phase; at 25 μM, its relative extent is about 2%. The inset in the bottom panel is a plot of the fraction fast phase for both inhibitors, showing a saturation of ~0.5 for terbutryn. Similar patterns were obtained with these inhibitors using chromatophores of *R. sphaeroides* (see below) or whole cells of *Rhodospirullum rubrum*.

The relative extent of the fast recombination phase observed in the presence of an inhibitor is usually taken (*4*, *11*) as the fraction of inhibited RCs undergoing $P^+Q_A^- \rightarrow PQ_A$ recombination ($t_{1/2} \approx 41$ ms in FJ2 chromatophores).

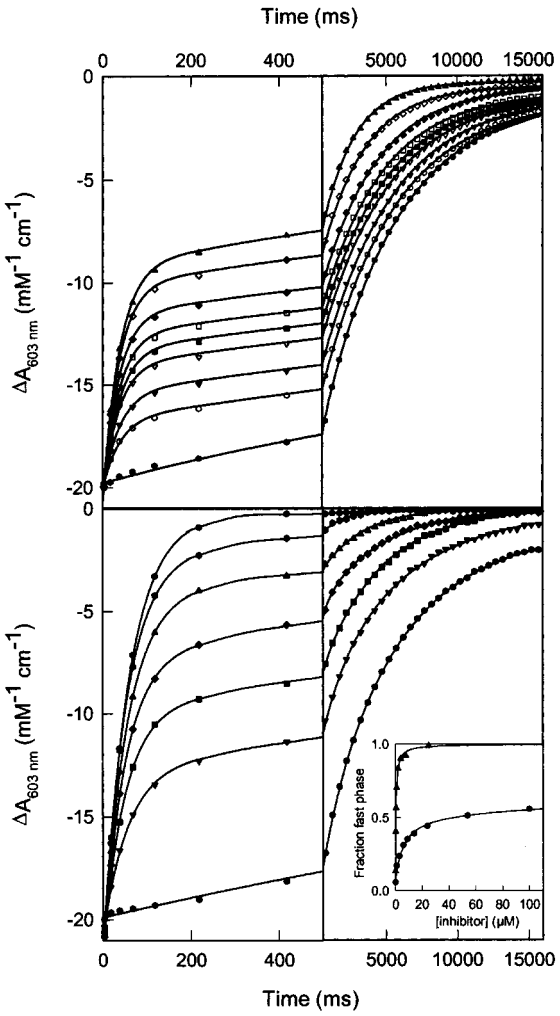

FIGURE 1: Recombination kinetics in the presence of terbutryn (top) or stigmatellin (bottom). The P^+ absorption changes following a saturating flash were monitored at 603 nm. Chromatophores of *R. capsulatus* (FJ2) at a RC concentration of 100 nM and pH 7.2. The inhibitor concentrations were 0, 1, 3, 6, 9, 14, 54, and 100 μM for terbutryn and 0, 0.25, 0.5, 1, 2, 8, and 25 μM for stigmatellin. The lines are fits of the data with a sum of three exponentials (one for the fast phase and two for the slow one). The $t_{1/2}$ of the fast phase was constant within experimental accuracy throughout the inhibitor range: 26 ms for terbutryn and 41 ms for stigmatellin. The inset (bottom panel) is a plot of the fraction fast phase vs inhibitor concentration, for terbutryn (●) and stigmatellin (▲).

The results obtained with triazines would then suggest a heterogeneity in inhibitor binding, with a much larger dissociation constant in a fraction of the RCs responsible for the remaining slow phase. The experiment shown in Figure 2 does not support this possibility. This figure shows the spectra in the near-IR region of the absorption change measured at 3 ms after a flash in the absence of inhibitor (●) or in the presence of 40 μM terbutryn (△) or 15 μM stigmatellin (□). At this time, inhibited RCs are still in the Q_A^- state whereas all uninhibited RCs have evolved to the Q_B^- state. In this spectral region, the major change is due to the $P^+ - P$ difference spectrum, with smaller contributions of spectral shifts due to the electrochromic effect of the anionic semiquinones Q_A^- and Q_B^- on neighboring pigments (mainly $BPhe_A$ for Q_A^- and $BPhe_B$ for Q_B^-). The latter species have significantly different spectra (*19*−*21*), allowing a discrimination of the semiquinones (which is far less easy

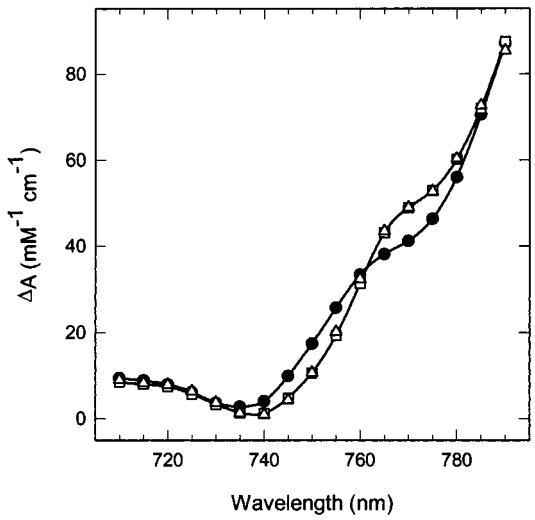

FIGURE 2: Near-IR spectra of the absorption change recorded 3 ms after a saturating flash. FJ2 chromatophores with (●) no addition, (□) 15 μM stigmatellin, and (△) 40 μM terbutryn (the stigmatellin and terbutryn data points are almost superimposed).

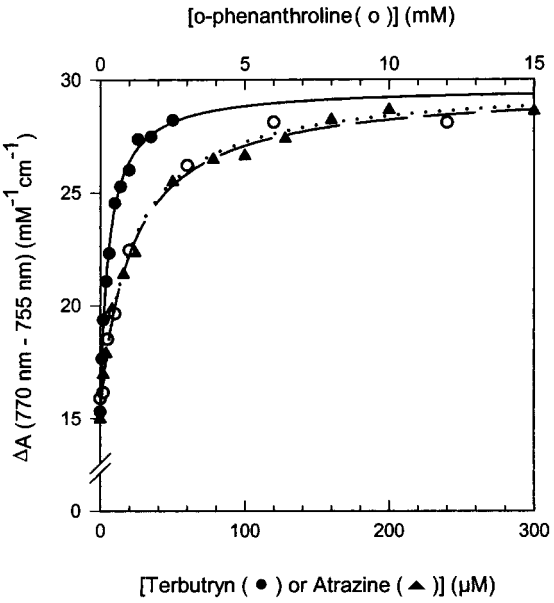

FIGURE 3: Difference of the absorption changes at 770 and 755 nm, recorded 3 ms after a saturating flash as a function of inhibitor concentration. FJ2 chromatophores with (●) terbutryn, (▲) atrazine, and (○) *o*-phenanthroline (upper horizontal scale). The lines are fits with eq 4.

in the blue and near-UV bands of the semiquinone spectra). These differences are readily observed when comparing the spectrum obtained in the absence of inhibitor ($P^+Q_B^- - PQ_B$) with that obtained in the presence of stigmatellin, expected to reflect $P^+Q_A^- - PQ_A$. The spectrum measured in the presence of terbutryn is superimposed with that of stigmatellin, although the relative extents of the slow phase observed during the decay are about 50 and 2%, respectively. This indicates that a few milliseconds after the flash, the fraction of inhibited RCs in the presence of 40 μM terbutryn is close to 100%, despite the large slow phase developing at later times.

We propose the following interpretation. The inhibited RCs (in the $P^+Q_A^-$I state immediately after the flash) are subject to a competition between the $P^+Q_A^-$ recombination and displacement of the inhibitor leading to the formation of $P^+Q_B^-$. The kinetic equations for this process are given in the Appendix (section 4). The displacement process involves the release of the inhibitor from the Q_B pocket (mostly controlled by the rate constant k_{off}), followed by UQ binding and electron transfer from Q_A^- to Q_B. The final equilibrium constant K''_2 (=$[Q_AQ_B^-]/[\text{total } Q_A^-]$) depends (see eq 7) on the inhibitor concentration and the apparent dissociation constant (K'_i) and on the electron-transfer apparent equilibrium constant K'_2 (=$[Q_AQ_B^-]/[Q_A^-Q_B]$). These "apparent equilibrium constants" encompass the effect of UQ binding. The constant K'_2 can be estimated (eq 3) from the recombination rate constants for $P^+Q_A^-$ and $P^+Q_B^-$, denoted k_{AP} and k'_{BP}, respectively. The observed rate constant k'_{BP} ($\approx$0.65 s^{-1} at pH 7.2) reflects the competition of a slow direct pathway [with a rate constant k_{dir} that we previously estimated to be $\sim$0.08 s^{-1} in FJ2 chromatophores (*16*)] and the indirect pathway via Q_A^- (*22*−*25*). The rate constant of the latter is thus k_{BP} (=$k'_{BP} - k_{dir}$). With a k_{AP} of $\approx$16.4 s^{-1} (corresponding to the 41 ms halftime of the decay in the presence of stigmatellin), one thus obtains a K'_2 of $\approx$100 (or 84 when omitting the correction for k_{dir}). The efficiency for inhibitor binding is thus decreased about 100-fold in the odd state so that nearly complete inhibitor displacement can take place over a broad range of inhibitor concentrations.

From a kinetic point of view, the displacement process is competing with the $P^+Q_A^-$ recombination, depending on the value of k_{off} compared with k_{AP}. The observed behavior can be understood on this basis, assuming that the k_{off} is of a magnitude similar to that of k_{AP} for terbutryn, somewhat smaller for atrazine and *o*-phenanthroline, and much smaller for stigmatellin. In agreement with this model, the rate of the fast phase observed with triazines ($t_{1/2}$ = 26 ms for terbutryn in FJ2) is faster than with stigmatellin because the effective rate constant is expected to be approximately $k_{AP} + k_{off}$ (see the Appendix, section 4).

Figure 3 shows titrations for the binding in the dark of several inhibitors, measured from the 3 ms absorption changes induced by a saturating flash at wavelengths (770 nm − 755 nm) where the spectral difference between Q_A^- and Q_B^- is largest. As noted above, the absorption change at 3 ms is that of $P^+Q_A^-$ in RCs with bound inhibitor and that of $P^+Q_B^-$ in uninhibited RCs. Thus, the 770 nm − 755 nm difference monitors the evolution from $P^+Q_B^-$ to $P^+Q_A^-$ as a function of inhibitor concentration. The fits with the binding law (eq 4) are satisfactory (a similar result may of course be obtained from a double-reciprocal plot, although with degraded accuracy) and allow determination of K'_i (see Table 1, column *a*).

In Figure 4 are shown plots of the relative extent of the fast phase versus the fraction of initially inhibited centers. A linear dependence is expected (eq 23), with a slope $k_{AP}/(k_{off} + k_{AP})$. The denominator can be estimated from the rate of the fast phase. Combining these two pieces of information, one obtains the value of k_{AP} in the presence of a given inhibitor and the value of k_{off}. Table 1 compiles the data thus obtained (columns *e* and *f*, respectively).

The apparent dissociation constant K'_i determined from experiments such as that of Figure 3 relates to inhibitor binding in the dark, with Q_A in its oxidized state, because it is measured a short time after the flash. According to Wraight (*4*), this constant, K'^D_i (D for dark), differs from that observed

Table 1: Data for Dissociation and Rate Constants of the Various Inhibitors

bacterium	inhibitor	$K'_i{}^D$ (μM)[a]	$K'_i{}^L$ (μM)[b]	$k_{AP}/(k_{AP}+k_{off})$[c]	$k_{AP}+k_{off}$ (s^{-1})[d]	k_{AP} (s^{-1})[e]	k_{off} (s^{-1})[f]	k_{off} (s^{-1})[g]
R. capsulatus	terbutryn	6.0	22,* 26**	0.50	26.0	13.0	13.0	12.2
	atrazine	19.0	30,* 52***	0.81	17.8	14.4	3.4	2.0
	o-phe	1000	3540*	0.86	20.0	17.2	2.8	0.8
	stig	0.37		0.97	16.9	16.4	–	0.033
R. sphaeroides	terbutryn	3.5	25,* 32**	0.68	17.3	14.3	3.0	1.5
	o-phe	360	450*	0.87	15.1	13.1	2.0	0.53
	stig				14.6			

[a] Determined as shown in Figure 3. The value for stigmatellin was corrected for the fraction of bound inhibitor. [b] One asterisk denotes a value determined from k_{slow} (as in Figure 5), i.e., in the presence of P^+. The data were corrected from k_{dir} for *R. capsulatus* but not for *R. sphaeroides*. Two asterisks denote a value determined (as in Figure 8) from the relaxed equilibrium in the presence of TMPD (i.e., in the presence of reduced P). Three asterisks denote a value determined, also in the presence of TMPD, from the dependence of the displacement rate on inhibitor concentration (eq 27, data from N. Ginet and J. Lavergne, manuscript in press in *Biochemistry*). [c] Slope of the plot of the fraction fast phase vs inhibited fraction (as in Figure 4). [d] Rate of the fast phase. [e] From columns *c* and *d*. [f] Difference of columns *d* and *e* (omitting the stigmatellin value because of low accuracy). [g] From the kinetics of inhibitor displacement in the presence of TMPD (as in Figure 6).

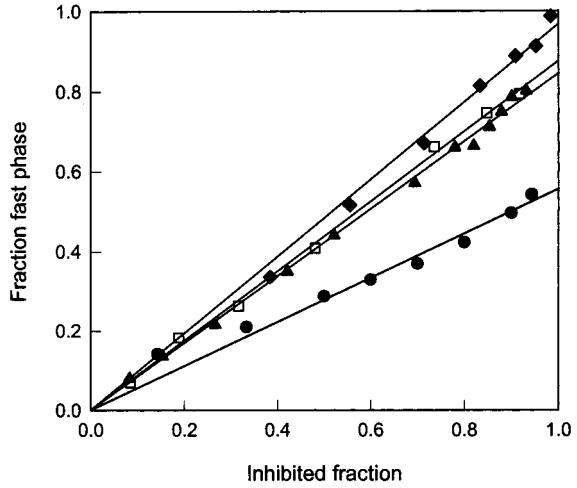

FIGURE 4: Plots of the fraction fast phase vs inhibited fraction (computed using the values of K'_i obtained as shown in Figure 3). FJ2 chromatophores. The fraction fast phase was corrected from the 3−10% contribution found in the absence of inhibitor: (●) terbutryn, (▲) atrazine, (□) *o*-phenanthroline, and (◆) stigmatellin. The slopes of the regression lines (possibly averaged from several experiments) are indicated in column 3 of Table 1.

in the presence of Q_A^-, denoted $K'_i{}^L$ (L for light) (see the Appendix, section 6). It is possible to estimate $K'_i{}^L$ from the dependence of the rate k_{slow} of the slow recombination phase on the inhibitor concentration. The rate of the slow phase is expected to increase linearly with the inhibitor concentration, according to eq 25. Such plots are shown in Figure 5. From the slope of the regression line, one can compute $K'_i{}^L$. This calculation uses the value of $k_{AP}/(k_{AP}+k_{off})$ obtained from Figure 4 (column *c* in Table 1) and the value of k_{BP} corrected from k_{dir}.

In chromatophores of *R. sphaeroides* CYC17 (bottom panel), the plots of k_{slow} versus *I* displayed two phases. This was observed both with terbutryn and (not shown) with *o*-phe. We have no explanation for this behavior (which was also observed in FJ2 chromatophores at lower pH). For terbutryn, the estimate of $K'_i{}^L$ from the initial slope is about 7 μM (compared with a K_i^D of ≈3.5 μM), whereas if $K'_i{}^L$ is computed from the linear regression in the high concentration range, a value of 25 μM is obtained. The latter value (featuring in Table 1) is in better agreement with that (denoted with two asterisks in Table 1, column *b*) estimated from the damping of semiquinone oscillations that will be described later.

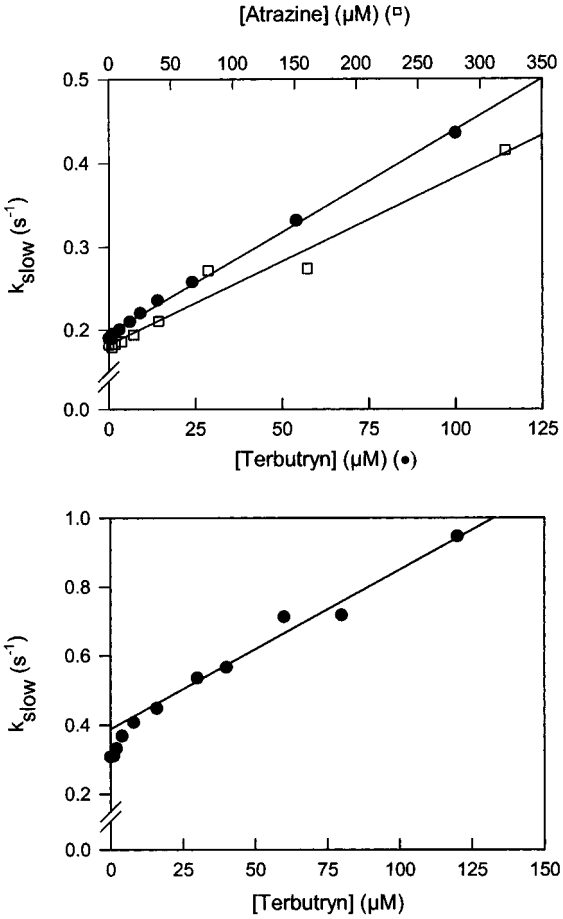

FIGURE 5: Plots of the rate of the slow recombination phase k_{slow} vs inhibitor concentration. Because the slow phase was generally better fitted using a sum of two exponentials, we used the overall $t_{1/2}$ and estimated k_{slow} as $\ln 2/t_{1/2}$: (top) FJ2 chromatophores with terbutryn (●) and atrazine (□) and (bottom) CYC17 chromatophores with terbutryn.

The kinetics of inhibitor displacement can be directly observed in the presence of a donor ensuring rapid reduction of P^+ so that the recombination pathway is essentially abolished. We used TMPD at a concentration of 1 mM. Except for experiments of short duration, the chromatophore suspension was kept anaerobic with a flow of argon and KCN was added to minimize TMPD autoxidation. The $t_{1/2}$ for P^+ reduction under such conditions was about 1 ms. Figure 6 shows the time course of absorption changes caused by two flashes spaced 4 s apart, in the presence of 20 μM terbutryn,

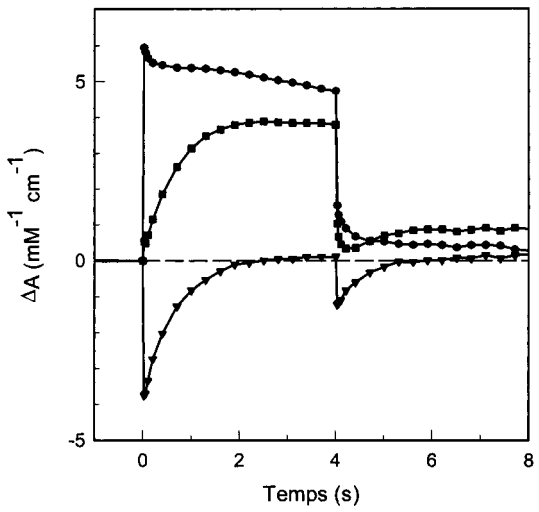

FIGURE 6: Kinetics of the absorption changes at 450 (●), 750 (▼), and 758 nm (■). Chromatophores from *R. sphaeroides* CYC17 at pH 7.2 in the presence of 1 mM TMPD and 5 mM KCN under anaerobic conditions. The sample was dark-adapted for at least 3 mn, ensuring almost total reoxidation of Q_B^-. Two flashes were fired (4 s apart). The kinetics at 750 and 758 nm were satisfactorily fitted as a single exponential with a $t_{1/2}$ of 455 ms.

in chromatophores of *R. sphaeroides*. The wavelengths were chosen for monitoring the total semiquinone [450 nm (●)] or, individually, Q_A^- [750 nm (▼)] and Q_B^- [758 nm (■)]. The negative change at 750 nm (an isosbestic wavelength for Q_B^- in this material) monitors the formation of Q_A^- after the first flash, decaying with a $t_{1/2}$ of 455 ms. The kinetics return to the baseline, showing that the decay of Q_A^- is essentially complete. A much smaller amount of initial Q_A^- is observed on the second flash, reflecting the presence of a fraction of centers in the even state when this flash is fired. At 758 nm (an isosbestic wavelength for Q_A^-), one observes the slow formation of Q_B^- after the first flash, concomitant with the disappearance of Q_A^-, and its destruction on the second flash. At 450 nm, both semiquinones have similar extinction coefficients. The conversion of Q_A^- to Q_B^- following the first flash is expressed by a roughly constant absorption level (the slow decay is presumably due to Q_B^- reoxidation by the oxidized TMPD). A sharp decay toward the baseline follows the second flash, reflecting the formation of quinol at the Q_B site. The binary pattern at 450 nm confirms that the displacement of the inhibitor has occurred during the dark interval between the flashes. The k_{off} for the displacement of several inhibitors measured (using eq 27) in experiments such as that of Figure 6 is indicated in Table 1 (column *g*). Qualitatively similar results were obtained with isolated RCs (not shown). For instance, with *R. capsulatus* RCs in the presence of 40 μM UQ-6, we observed a half-time of 330 ms for inhibitor displacement with 120 μM atrazine.

A marked difference was observed between *R. capsulatus* and the other bacteria that were investigated (*R. sphaeroides* and *Rubrivivax gelatinosus*), concerning the IR changes associated with Q_B^- in experiments such as that of Figure 6. Analysis of this phenomenon shows that it is due to a specific spectral effect caused by the binding of triazines to the Q_B pocket in this bacterium. This issue does not affect the present interpretations, and will be dealt with elsewhere (N. Ginet and J. Lavergne, manuscript in press in *Biochemistry*).

The much slower k_{off} of stigmatellin could not be measured in the same manner because of the absorption drifts on a long time scale. We measured the recovery kinetics of the P^+ change induced by a second flash fired Δt after the first one (not shown) and obtained a half-time of 21 s ($k_{off} \approx 0.033\ s^{-1}$).

The results described so far indicate that, at an appropriate inhibitor concentration, one can have an almost complete inhibitor binding in the dark (on "even state" RCs) and an almost complete inhibitor displacement after one flash (on "odd state" RCs). This means that the overall functioning of the two-electron gate is preserved under such conditions, provided the time spacing between odd- and even-numbered flashes is long enough to allow completion of the displacement process (as originally found in ref *13*). This is easily achieved with inhibitors that have a relatively large k_{off}, such as terbutryn, atrazine, or *o*-phenanthroline. This situation allows the design of a "phase-resetting" procedure as we will now describe. Let us consider the effect of a pair of flashes, spaced about 10 ms apart, on even or odd state centers. This time spacing is long with respect to P^+ reduction by TMPD. It is also sufficient to complete the formation and release of quinol in centers which were initially in the $Q_AQ_B^-$ state.[2] Thus, before the second flash of the pair, these centers are in the open states PQ_AQ_B and PQ_AI. The fraction of the latter depends on the rate of the binding equilibrium ($\approx k_{on}I$ when $I \gg K'_i$). Assuming for instance an inhibitor concentration of $10K'_i$, one has a $k_{on}I$ of $10k_{off}$, and thus half-times of 57, 460, and 870 ms for terbutryn, atrazine, and *o*-phenanthroline, respectively (using the figures in column *g* for FJ2 in Table 1). Therefore, at 10 ms, most centers have not yet bound the inhibitor. The second flash of the pair will result (after P^+ reduction) in states $PQ_AQ_B^-$ and, for a minor fraction, PQ_A^-I. The inhibitor displacement in the latter leads as well to state $PQ_AQ_B^-$ in a few seconds. Therefore, the centers initially in the odd state $Q_AQ_B^-$ are restored to the same state a few seconds after the flash pair. On the other hand, centers initially in the PQ_AI state are converted to state $P^+Q_A^-I$ (rapidly followed by state PQ_A^-I) after the first flash. Because the time lapse between the two flashes is short with respect to the inhibitor displacement process, these centers are still closed and unmodified by the second flash.

The outcome of the above procedure is to set almost all centers in the odd state, irrespective of their initial state. This is illustrated in Figure 7. In the experiment of the top panel, the illumination pattern consisted of alternating a pair of resetting flashes and a single flash with a time spacing of 3 s. The 450 nm absorption changes show the semiquinone formation caused by each flash pair and its destruction caused by the single flash. The efficiency of the resetting procedure is demonstrated by the absence of damping of the binary oscillation and by its amplitude. The level reached after each resetting flash pair corresponds to more than 0.9 semiquinone per center. The amplitude of the oscillation is somewhat smaller (about 0.77 semiquinone). In the bottom panel, the chromatophores were first submitted to a series of 20 single flashes, to mix odd and even states due to the damping. A

[2] Quinol release occurs in the 1 ms time range, as estimated from the lag for reduction of cytochrome b_{561} in the $b-c_1$ complex (*1*). Due to the large UQ/RC ratio in chromatophores [about 25 (*1*, *2*)], the binding of UQ probably also occurs in the same time range (*3*).

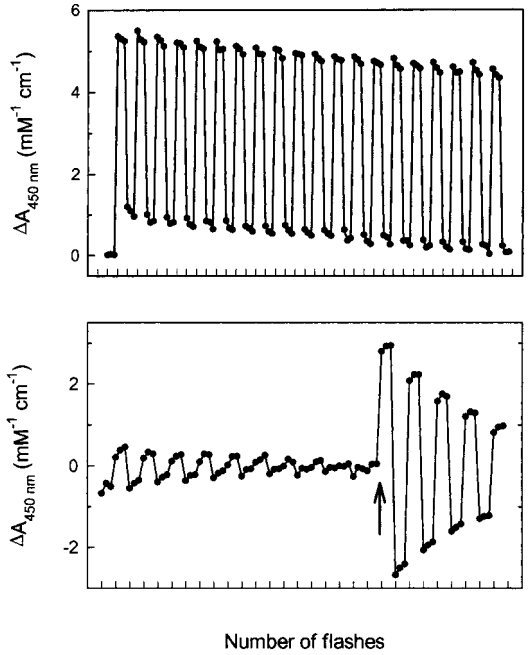

FIGURE 7: Illustration of the resetting procedure showing semiquinone oscillations monitored at 450 nm. FJ2 chromatophores in the presence of 60 μM atrazine, 1 mM TMPD, and 5 mM KCN under anaerobic conditions: (top) repetitive illumination after a long dark adaptation period, with a pair of saturating flashes spaced 10 ms apart, a 3 s delay, one single flash, a 3 s delay, and so forth; and (bottom) illumination with a series of 20 single flashes, a pair of resetting flashes spaced 10 ms apart (arrow), and eight single flashes (the flash spacing is 3 s throughout).

pair of resetting flashes was then triggered (arrow), followed by continuation of the train of single flashes. The flash pair resulted in a very efficient phase resetting, placing almost all centers in the odd state. The amplitude of the first oscillation after the resetting (i.e., the amount of semiquinone destroyed by the next flash) corresponds to 0.9 semiquinone per RC.

We have described above a method for estimating $K'_i{}^L$ from the rate of the slow phase of recombination. This estimation actually relates to centers in state $P^+Q_A^-$. Alternatively, one can measure the apparent dissociation constant for centers in state PQ_A^-. This was carried out in the presence of TMPD, by estimating the equilibrium fraction of odd state centers in the Q_A^- state after completion of the inhibitor displacement. A sensitive technique (*26*, *39*) is to measure the damping of semiquinone oscillations during a series of saturating flashes spaced a few seconds apart. In this procedure, it is essential to prevent accumulation of oxidized TMPD which can reoxidize a significant fraction of the semiquinones during the relatively long interval between flashes. Thus, the duration of individual experiments was kept short, and control tests that were run without inhibitor showed that under the conditions we used, the damping was not increased due to the low flashing rate required for these experiments. When using *R. capsulatus* chromatophores, semiquinone oscillations were recorded at 450 nm rather than in the IR region, because of the spectral interference mentioned earlier due to inhibitor binding in this material. At this wavelength, an absorption change due to the oxidation of TMPD (resulting from P^+ reduction) is superimposed on the semiquinone signal. This was taken into account in the treatment of the data as explained in the legend of Figure 8.[3] Panel A in this figure shows the raw data and panel B the successive absorption changes caused by each flash, with sign-inverted on even-numbered flashes. The fitting of these data yields the apparent equilibrium constant K''_2 (eq 7),

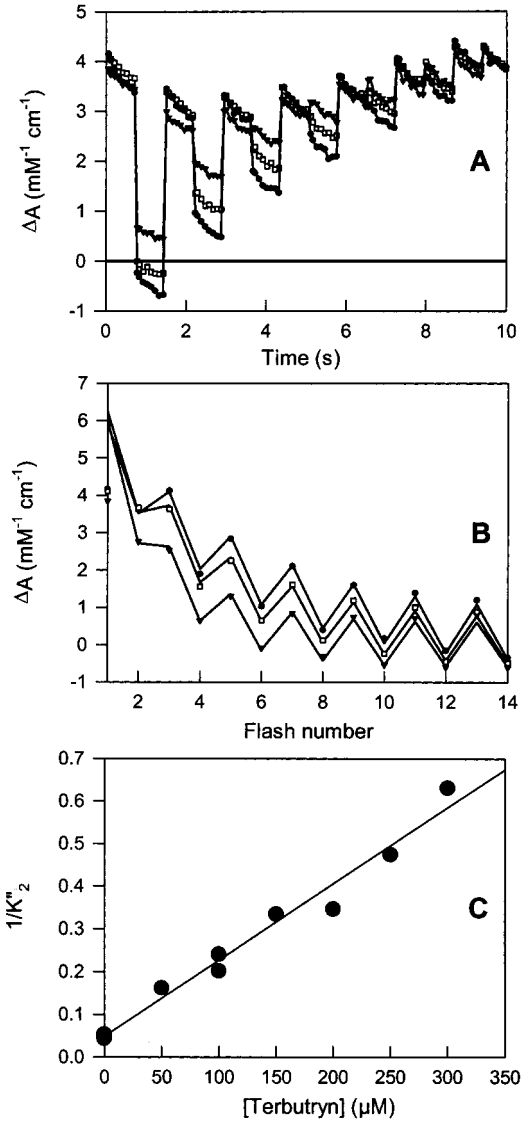

FIGURE 8: Damping of the semiquinone oscillations for various concentrations of terbutryn. FJ2 chromatophores in the presence of 1 mM TMPD. (A) Absorption changes at 450 nm during a series of 14 saturating flashes spaced 720 ms apart, in the presence of 100 (●), 200 (□), and 300 μM (▼) terbutryn. The "first" flash was a resetting flash pair. Tests for ensuring that no artifactual damping was present (saturating character of the actinic flash and absence of actinic effect of the measuring light) were described in ref *39*. (B) Successive absorption changes caused by each flash with sign-inverted on even-numbered flashes. The lines connect the points obtained from a fit of the data, using the function $\Delta An = A \exp(-kn) + (-1)^n B$, with A, B, and k as adjustable parameters. The introduction of B is required because of the contribution due to TMPD oxidation.[3] The apparent equilibrium constant $K''_2 = e^{-k}/(1 - e^{-k})$ (see ref *39*). The failure of the fit on flash 1 is due to the singularity introduced by the resetting flash pair. (C) A plot of $1/K''_2$ vs the terbutryn concentration, used to determine $K'_i{}^L$ according to eq 8.

[3] The contribution of TMPD is not constant during the flash sequence, because centers in the Q_A^- state are photochemically inactive. Nevertheless, the fitting equation is correct: the TMPD change is split between a constant part (B) and an oscillating part present in A, with the same damping as semiquinone oscillations.

according to the procedure described in ref *39*. Panel C shows the plot of $1/K''_2$ versus *I* used for determining K'^{L}_i according to eq 8. The value thus obtained for terbutryn (featured in column *b* of Table 1 with two asterisks) is 26 μM, somewhat larger than that (22 μM) obtained in the presence of $P^+Q_A^-$. It is noteworthy that the intercept of the plot in panel C (i.e., the value of $1/K'_2$ in the absence of inhibitor) corresponds to a much smaller value of K'_2 ($\approx$5-fold) than that estimated from recombination kinetics. Indeed, as investigated in ref *39*, we observed a marked effect of the state of P on this equilibrium constant.

DISCUSSION

The interpretative framework of competitive binding of quinones and inhibitors on the Q_B pocket has been established for many years (*8*−*11*). In the work presented here, we have focused on dynamical aspects. It shows that triazines and *o*-phenanthroline have a relatively rapid turnover in chromatophores (especially those from *R. capsulatus*) so that the unbinding rate of the inhibitor is not negligible with respect to the rate of $P^+Q_A^-$ recombination. As a consequence, the fast phase observed at some inhibitor concentrations reflects a competition between the recombination of state $P^+Q_A^-I$ and inhibitor release, leading to the formation of state $P^+Q_B^-$. Under such conditions, the extent of the fast phase is not a direct measurement of the fraction of centers with bound inhibitor, as is usually assumed.[4] This is particularly obvious with terbutryn, with which as much as 50% slow phase (in *R. capsulatus*) is observed at concentrations which saturate inhibitor binding in the dark. Consistent with this interpretation, the rate of the fast phase is markedly faster than that of $P^+Q_A^-$ recombination (k_{AP}), reflecting in fact the sum $k_{AP} + k_{off}$.

A reliable estimation of the fraction of inhibited centers can be obtained by measuring the flash-induced near-IR absorption changes at wavelengths where the Q_A^- and Q_B^- spectral differences are largest. We could in this way estimate the fraction of inhibited centers present at a short time after a saturating flash and measure the apparent dissociation constant K'^{D}_i (eq 5). Moreover, recording the time courses of these changes in the presence of a rapid donor to P^+ allows a direct monitoring of the inhibitor release, reflected by the concomitant decay of Q_A^- and formation of Q_B^-. These kinetics allow the measurement of k_{off}, using eq 27.

We now comment the results compiled in Table 1. The affinity of the assayed inhibitors for the RC ranks in the order stigmatellin, terbutryn, atrazine, and *o*-phenanthroline. This goes for both *R. capsulatus* and *R. sphaeroides*, with 2−3-fold larger dissociation constants in the former for terbutryn and *o*-phenanthroline. The affinity ranking does not reflect an exclusive effect from k_{off} or k_{on}. For instance, whereas the low K'^{D}_i of stigmatellin is associated with a very slow k_{off}, terbutryn, which has the second lowest K'_i, has the largest k_{off}. It should be kept in mind, however, that these affinities also depend on the partition coefficients of the inhibitors in the membrane phase. Compared with chromatophores, we obtained qualitatively similar results with isolated RCs from *R. capsulatus* and *R. sphaeroides* regarding the ranking of dissociation constants and release rates (data not shown).

For inhibitors which have a relatively rapid release rate (i.e., all except stigmatellin), we could estimate the k_{off} from the acceleration and truncation of the fast recombination phase (Table 1, column *f*; see Appendix section 4) and compare it with the value derived from the inhibitor displacement kinetics in the presence of TMPD (column *g*). The estimates in column *f* are all greater (by a factor ranging from 1.1 to 3.8) than those in column *g*. This effect is particularly significant for *o*-phenanthroline. Barring some systematic error in our procedures, this suggests an effect of the presence of P^+ that would tend to accelerate the release of the inhibitor. The recombination data of columns *c* and *d* also give access to the specific k_{AP} in the presence of a given inhibitor (column *e*). These values generally agree within experimental accuracy with that observed with stigmatellin, except perhaps in the case of terbutryn in *R. capsulatus*, where the recombination rate appears significantly slower.

Although the equilibrium constant K'_2 ($=[Q_AQ_B^-]/[Q_A^-Q_B]$) is about 5-fold smaller in the presence of P than in the presence of P^+ (*39*), one can still adjust the inhibitor concentration so as to almost saturate inhibitor binding in the dark and obtain almost complete inhibitor displacement after one flash in the presence of a rapid donor to P^+. This contrast is in fact enhanced by another phenomenon, namely, the increase in the inhibitor dissociation constant in the presence of Q_A^-, which is discussed below. The outcome is that one can have an uninhibited overall turnover of the two-electron gate, provided the flash spacing is long enough. There is, however, one conspicuous modification; the rate of electron transfer from Q_A^- to Q_B has become limited by the inhibitor release so that it is shifted from tens to hundreds of microseconds to tens to hundreds of milliseconds. On the other hand, the rate of the second electron transfer $Q_A^-Q_B^- \rightarrow Q_AQ_BH_2$ is unchanged [completed in a few hundreds of microseconds (data not shown)]. This opens interesting means for handling the two-electron gate. A frequently encountered problem when studying this system is to control the fraction of Q_B^- present in the dark. As illustrated in Figure 7, it is very easy to reset the phase of the system by giving a pair of appropriately spaced saturating flashes. The optimum time spacing of the flash pair is determined by the following constraints. It must be longer than the time required for P^+ reduction and also longer than the time required for the electron transfer from Q_A^- to Q_B^- in odd state centers. On the other hand, it must be short with respect to the inhibitor displacement rate. This technique should prove quite useful for studying the two-electron gate (e.g., quinol formation upon the second electron transfer), because it allows a repetitive procedure without damping. From a more speculative point of view, the Q_B system may be seen as a molecular binary memory; we now have a technique which allows optical resetting of this device.

In previous studies, Wraight and co-workers concluded that the binding properties of the Q_B pocket (in chromatophores or isolated RCs of *R. sphaeroides*, with added UQ in the latter material) differed markedly depending on the state of Q_A. The dissociation constants were labeled "D" for dark in the presence of Q_A and "L" for light in the presence of

[4] In ref *4*, Wraight and co-workers were quite aware that the rapid release rate of terbutryn was responsible for the remaining fraction of the slow phase at high inhibitor concentrations. Nevertheless, the inhibition was assessed from the absolute extent of the fast phase rather than from its relative extent (i.e., assuming a slope of 1 in Figure 4). The K'_i thus obtained was overestimated by a factor of 1.5−2.

Q_A^-. This group actually reported two effects. First, the E_m of the Q_A/Q_A^- couple was shifted to lower potentials when quinone was added to isolated RCs incorporated into liposomes (*8*). In the potential range where this couple titrates in, the added quinone is essentially in its reduced (quinol) form. The observed effect thus means that quinol binding to the Q_B pocket is destabilized in the presence of Q_A^- (i.e., increased K_q for the quinol form). Second, from the analysis of the recombination kinetics in the presence of inhibitor (terbutryn) and added quinone, Wraight (*4*) inferred that the inhibitor binding was also disfavored in the presence of Q_A^- (therefore, $K'_i{}^L > K'_i{}^D$). The apparent inhibitor dissociation constant includes the effect of the competition from quinone (eq 5). Therefore, the observed effect may be predominantly due to a change in K_i (thus, $K_i^L > K_i^D$) or predominantly due to K_q (if $K_q^L < K_q^D$ for the oxidized UQ) or may arise from some combination of both. Clearly, if $K_q^L < K_q^D$, this implies that the presence of Q_A^- has opposite effects on the binding of quinone (favored) and on that of quinol (disfavored), which would facilitate the turnover of the Q_B pocket. In a later study of the binding of labeled inhibitors to isolated RCs, Diner et al. (*11*) investigated this issue and found no difference between K_i^L and K_i^D for terbutryn. In this experiment, no secondary quinone was present, so the data are relevant to the true dissociation constant K_i, not to the apparent K'_i.

Wraight's analysis rested on a guessed expression for k_{slow} (eq 24) which assumes that the slow phase proceeds at quasi equilibrium with respect to inhibitor binding (i.e., that the relative amount of state $P^+Q_A^-I$ is close to its equilibrium value). This assumption is quite wrong, however, because state $P^+Q_A^-I$ represents an effective kinetic sink (the slowest rate constants in the system are those for inhibitor binding and release, not k_{AP}). In the Appendix (section 4), we have derived an analytical solution for the recombination kinetics in the presence of an inhibitor so that we have an "exact[5]" expression (eqs 16−21) and a good approximate one for k_{slow} (eq 25). The dependence of k_{slow} on I is much steeper in eq 24 than in eq 25, so one may wonder whether Wraight's conclusion about $K'_i{}^L$ being greater than $K'_i{}^D$ was not entirely due to his overestimation of the theoretical acceleration of k_{slow} as a function of I.

The work presented here allows a reassessment of this issue. The inhibitor titration of the amount of $P^+Q_A^-$ present a few milliseconds after a flash based on the near-IR spectral differences between $P^+Q_A^-$ and $P^+Q_B^-$ (see Figures 2 and 3) gives an unambiguous determination of $K'_i{}^D$. Although made in the presence of Q_A^-, this measurement takes place in a time range much shorter than k_{off}^{-1} so that one essentially monitors the amount of inhibitor bound before the flash, in state PQ_A. For *R. capsulatus* FJ2 chromatophores, we obtained in this manner $K'_i{}^D$ values of ≈6 and ≈19 μM for terbutryn and atrazine, respectively. For the measurement of $K'_i{}^L$, several methods were used. The first one (illustrated in Figure 5) is based on the slope of k_{slow} versus I, using eq 25, and relates to centers in the state $P^+Q_A^-$. This yielded $K'_i{}^L(P^+)$ values of ≈22 and ≈30 μM for terbutryn and atrazine, respectively. We also estimated $K'_i{}^L$ in the presence of reduced P. For terbutryn, this was obtained from the damping of semiquinone oscillations (Figure 8), yielding a $K'_i{}^L(P)$ of ≈26 μM. This method could not be used reliably with atrazine, due to its slower displacement kinetics. We thus used eq 27 and derived a $K'_i{}^L(P)$ of ≈52 μM from the dependence of the displacement rate on atrazine concentration (data of N. Ginet and J. Lavergne, manuscript in press in *Biochemistry*). The outcome (see Table 1) is that $K'_i{}^D < K'_i{}^L(P^+) < K'_i{}^L(P)$. The effect of Q_A^- is largest with terbutryn (about 4 in FJ2 and 7 in *R. sphaeroides* CYC17). A significant effect was also found for *o*-phe in FJ2 (3.5), at variance with CYC17. We thus confirm, on the basis of independent evidence and a more correct treatment of the data, the effect reported by Wraight and co-workers of a decreased affinity for triazines in the presence of Q_A^-. The analysis of interactions between the acceptor and donor side presented in ref *39* predicts a very different behavior of stigmatellin, with regard to the effect of the state of P. Whereas the oxidation of P causes an increase in $K'_i{}^L$ for triazines, we expect a large (≈10-fold) decrease for stigmatellin. We proposed that the differences between stigmatellin and terbutryn arise from different binding sites: stigmatellin (*6*, *27*) is known to bind at the proximal site of the Q_B pocket, whereas triazines bind at a more distal position (*27*, *28*).

The finding that the apparent dissociation constant of terbutryn is increased in the presence of Q_A^- is not necessarily in conflict with that of Diner et al. (*11*) (i.e., $K_i^D = K_i^L$ in Q_B depleted isolated RCs). These results can be reconciled if the effect of Q_A^- is primarily due to its influence on UQ binding, i.e., if $K_q^L < K_q^D$. In agreement with this view, we found (N. Ginet and J. Lavergne, manuscript in press in *Biochemistry*) that the effect on K'_i is not due to an increased k_{off} in the presence of Q_A^-, but entirely to a change in the apparent k_{on}. An implication of this proposal is that the amino acid ligand(s) specifically responsible for the increased affinity of UQ in the presence of Q_A^- is not involved in the binding of terbutryn.

The redox titrations of Q_A in the presence or absence of secondary quinone and inhibitor (*o*-phenanthroline) reported by Wraight (*8*) also support this picture. If $K_i^L > K_i^D$ (true dissociation constants), then the presence of inhibitor (in the absence of secondary UQ) should stabilize the oxidized form Q_A, and thus decrease the E_m of the Q_A/Q_A^- couple. In contrast, the inhibitor alone had no effect on the midpoint potential of Q_A. In the presence of UQ, which decreased the E_m of Q_A when added alone, the inhibitor reversed the effect. We have, however, the following problem with respect to the data reported in this work. The above titration results would predict an increased $K'_i{}^L$ for *o*-phe in *R. sphaeroides*, which we did not find (at variance with FJ2). It is thus possible that our estimate of the $K'_i{}^L$ for *o*-phe in CYC17 is faulty, perhaps due to the biphasic character of the k_{slow} versus I plot. Alternatively, the problem may have to do with the strains. While the values of $K'_i{}^D$ that we obtained for terbutryn or atrazine match very well the values reported by Stein et al. (*4*) for *R. sphaeroides* R-26 or Ga cells, our value for *o*-phe in CYC17 is about 10-fold larger than those reported by Stein et al.

Together with the opposite effect found by Wraight for quinol binding ($K_q^L < K_q^D$), this suggests that the primary quinone modulates the binding properties of the Q_B pocket

[5] "Exact" under the assumption that the system is in quasi equilibrium with respect to quinone binding (and also that $K'_i \gg$ [RC] so that the free and total inhibitor concentrations are almost equal).

so as to enhance the turnover rate for UQ reduction, favoring the release of reduced quinol and the binding of oxidized quinone when an electron is available on Q_A^-. It is noteworthy that the interdependence of the two quinone sites has also been emphasized from electrostatic calculations (*29*, *30*) and experiments on the pH dependence of proton binding (*31*) or of the ΔE_m between Q_A and Q_B (*30*). Interactions between the state of Q_A and the binding properties of the Q_B pocket have also been found in PS II. In PS II membranes, Knaff (*32*) reported that *o*-phenanthroline raises the midpoint potential of Q_A by 70 mV and Krieger-Liszkay and Rutherford (*33*) found that phenolic herbicides lower the E_m of Q_A by 45 mV while DCMU raises it by 50 mV. Thus, *o*-phenanthroline and DCMU affect the E_m of Q_A in PS II in the same manner as *o*-phenanthroline and (presumably) terbutryn in bacterial RCs. The mechanism may not be the same, however, because Krieger-Liszkay and Rutherford found no change in the midpoint potential of Q_A when removing the PQ pool, at variance with Wraight's result in bacterial RCs.

The long-range interactions controlling the properties of the Q_B site either from Q_A^- (this paper) or from P^+ (*39*) are of interest in several respects. They highlight the involvement of rearrangements that go beyond simple electrostatic interactions. These interactions are probably functionally important. According to the analysis presented here, the changes caused by Q_A^- appear to facilitate the Q_B turnover, by favoring quinone binding and quinol release. They may also play a role in the gating process believed to control the reduction of Q_B. It is likely that these effects are mediated by the protonation state of amino acids of the Q_B pocket (such as Glu L212), as in models proposed by several groups (*31*, *34*−*36*). An attractive possibility is a role of the His−Fe−His complex as a connecting link between the two quinone sites (*34*, *37*, *38*).

APPENDIX

(1) Recombination Rate of $P^+Q_B^-$. We consider the equilibria

$$P^+Q_A^- \overset{K_q}{\rightleftharpoons} P^+Q_A^-Q_B \overset{K_2}{\rightleftharpoons} P^+Q_AQ_B^-$$

showing, from left to right, the state with the Q_B pocket empty, occupied by an oxidized quinone, and occupied with semiquinone. For brevity, we denote the fractions of these species *X*, *Y*, and *Z*, respectively. K_q ($=X/Y$) is the apparent dissociation constant of UQ on the Q_B site (this is a shorthand notation for the true dissociation constant over the concentration of pool UQ which is assumed to be constant). In all likelihood, in chromatophores, $K_q \ll 1$, because of the large excess of UQ. K_2 ($=Z/Y$) is the equilibrium constant for electron transfer between Q_A and Q_B.

The fraction of RCs with Q_A^- is

$$X + Y = \frac{1}{1 + K'_2} \tag{1}$$

with

$$K'_2 = \frac{K_2}{1 + K_q} \tag{2}$$

If one assumes that the direct recombination from the $P^+Q_B^-$ state proceeds at a negligible rate with respect to the route going through Q_A^-, the rate constant for the decay of $P^+Q_B^-$ is

$$k_{BP} = k_{AP}\frac{1}{1 + K'_2} \tag{3}$$

where k_{AP} is the rate constant for $P^+Q_A^-$ recombination.

(2) Inhibitor Fixation on Even State Centers. We consider the scheme

$$Q_AI \underset{k_{on}I}{\overset{k_{off}}{\rightleftharpoons}} Q_A \overset{K_q}{\rightleftharpoons} Q_AQ_B$$

showing, from left to right, the states with bound inhibitor, an empty Q_B pocket, and bound UQ. We denote the fractions of these species *W*, *X*, and *Y*, respectively. K_i ($=k_{off}/k_{on}$) is the dissociation constant of the inhibitor. At equilibrium, the fraction of inhibited RCs is

$$W = \frac{1}{1 + K'_i/I} \tag{4}$$

where

$$K'_i = K_i\frac{1 + K_q}{K_q} \tag{5}$$

In these expressions, *I* denotes the concentration of free inhibitor. When K'_i is large with respect to the RC concentration (i.e., for all inhibitors used in this study, except stigmatellin), *I* is very close to the total inhibitor concentration.

The primed equilibrium constants K'_2 (eq 2) and K'_i (eq 5) are apparent constants which encompass the effect of the binding equilibrium of UQ at the Q_B site.

(3) Inhibitor Fixation on Odd State Centers. We have now

$$Q_A^-I \underset{k_{on}I}{\overset{k_{off}}{\rightleftharpoons}} Q_A^- \overset{K_q}{\rightleftharpoons} Q_A^-Q_B \overset{K_2}{\rightleftharpoons} Q_AQ_B^-$$

The fractions of the states shown from left to right are denoted *W*, *X*, *Y*, and *Z*, respectively. At equilibrium, the fraction of RCs with Q_A^- is

$$[Q_A^-] = W + X + Y = \frac{1}{1 + K''_2} \tag{6}$$

with

$$K''_2 = \frac{K'_2}{1 + I/K'_i} \tag{7}$$

Rearranging eq 6, one obtains

$$\frac{1}{K''_2} = \frac{[Q_A^-]}{1 - [Q_A^-]} = \frac{1}{K'_2} + \frac{I}{K'_2K'_i} \tag{8}$$

This predicts a linear dependence on *I* of the ratio of closed-to-open RCs with the intercept $1/K'_2$ and the slope $1/(K'_2K'_i)$.

(4) Recombination in the Presence of Inhibitor. The appropriate scheme is now

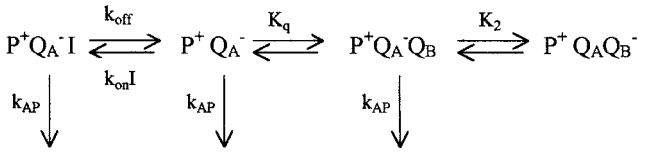

We denote as before the relative fractions *W*, *X*, *Y*, and *Z*, respectively. We assume that the equilibria involving UQ binding and electron transfer are fast with respect to that of inhibitor binding and recombination kinetics. The three rightmost states will then be in equilibrium and can be expressed as fractions of their sum *S* (=*X* + *Y* + *Z*). One has thus

$$X = S\frac{K_q}{1 + K_q + K_2}$$

$$Y = S\frac{1}{1 + K_q + K_2} \quad (9)$$

$$Z = S\frac{K_2}{1 + K_q + K_2}$$

The kinetic equations are

$$\frac{dW}{dt} = k_{on}IX - (k_{AP} + k_{off})W = k_{on}I\frac{K_q}{1 + K_q + K_2}S - (k_{AP} + k_{off})W \quad (10)$$

$$\frac{dS}{dt} = k_{off}W - k_{AP}(X + Y) - k_{on}IX = -\frac{k_{AP}(1 + K_q) + k_{on}IK_q}{1 + K_q + K_2}S + k_{off}W \quad (11)$$

This is a system of the form

$$\frac{dW}{dt} = \alpha S + \beta W \quad (12)$$

$$\frac{dS}{dt} = \gamma S + \delta W \quad (13)$$

where the coefficients α, β, γ, and δ can be read in eqs 10 and 11.

Solving eq 13 for *W* and inserting into eq 12, one obtains

$$\frac{d^2S}{dt^2} - (\beta + \gamma)\frac{dS}{dt} + (\beta\gamma - \alpha\delta)S = 0 \quad (14)$$

The solution of eq 14 is of the form

$$S(t) = S_1 \exp(r^+t) + S_2 \exp(r^-t) \quad (15)$$

where r^+ and r^- are the solutions of the algebraic trinome homologous to eq 14:

$$r^{\pm} = {}^1/_2(R \pm \sqrt{\Delta}) \quad (16)$$

with

$$R = -k_{AP} - k_{off} - \frac{K_q(k_{AP} + k_{on}I) + k_{AP}}{1 + K_q + K_2} \quad (17)$$

$$\Delta = \left[k_{AP} + k_{off} - \frac{K_q(k_{AP} + k_{on}I) + k_{AP}}{1 + K_q + K_2}\right]^2 + 4\frac{K_q k_{on} I k_{off}}{1 + K_q + K_2} \quad (18)$$

Using the apparent equilibrium constants, K'_2 and K'_i (eqs 2 and 5), this can be rewritten

$$R = -k_{AP}\left(1 + \frac{1}{1 + K'_2}\right) - k_{off}\left[1 + \frac{I}{K'_i(1 + K'_2)}\right] \quad (19)$$

$$\Delta = \left\{k_{AP}\frac{K'_2}{1 + K'_2} + k_{off}\left[1 - \frac{I}{K'_i(1 + K'_2)}\right]\right\}^2 + 4I\frac{k_{off}^2}{K'_i(1 + K'_2)} \quad (20)$$

We are interested in the decay of P^+, namely, the sum $W + S$. Both terms have the same exponential factors as *S*, so

$$[P^+](t) = A \exp(r^+t) + (1 - A) \exp(r^-t) \quad (21)$$

where the initial fraction of P^+ was set equal to 1 (saturating flash). Coefficient *A* (this is the fraction of the slow phase) can be determined by setting the initial fraction of *W* to its equilibrium value W_0 in the dark (eq 4) (then $S_0 = 1 - W_0$) and solving the equation obtained for the initial derivative of $[P^+]$ from eqs 21 and 10 and 11. One obtains

$$A = \frac{1}{2} - \frac{R}{2\sqrt{\Delta}} - \frac{k_{AP}}{\sqrt{\Delta}(1 + K'_2)}(1 + W_0K'_2) \quad (22)$$

Notice that the K'_i and k_{off} featured in the expressions of *R* and Δ (eqs 19 and 20) relate to the dissociation of the inhibitor in the presence of Q_A^-, whereas in W_0 (eq 4), the equilibrium occurs in the presence of Q_A. If the redox state affects inhibitor binding (see section 6 below), this should be taken into account when dealing with eq 22.

Several useful approximations can be derived and checked for accuracy using the above exact formulas and the set of constants in Table 1. The rate of the fast phase is close to $k_{AP} + k_{off}$. This agrees within 0.1% with the exact value, except for terbutryn (because of the large k_{off}) where the maximum discrepancy is about 1%. A good approximation for the relative amplitude of the fast phase is

$$1 - A \approx W_0\frac{k_{AP}}{k_{AP} + k_{off}} \quad (23)$$

This is verified within 3% (the exact value is systematically smaller than the approximated one). With regard to the rate of the slow phase ($-r^+$), the guesswork for an approximate expression is more tricky. It might be thought [see Wraight (*4*)] that the slow phase represents the decay of the totally equilibrated system, where $X/W = K'_i/I$. Its rate would then be approximately

$$k_{slow} \approx k_{AP}\frac{1}{1 + K''_2} \quad (24)$$

where K''_2 is given by eq 7. This quasi equilibrium treatment implies, however, that the decay rate is slow with respect to

the effective equilibration between *W* and *X*. This condition is far from being met for any of the inhibitors investigated in this study (even for terbutryn, although its turnover rate is highest), and the discrepancy between eq 22 and the exact value of the slow rate computed from eq 16 is very large. For instance, if one uses the set of constants in Table 1 and computes the slow rate $I/K'_i = 5$, the (k_{slow} from eq 22)/(k_{slow} from eq 16) ratio is 1.7 for terbutryn, 3.1 for *o*-phenanthroline, and 5.4 for stigmatellin. A much better approximation for k_{slow} can be derived in the following way. After completion of the fast phase, the fraction of centers in state $P^+Q_A^-I$ (=*W*) is very low so that the relative amount of state $P^+Q_A^-$ (=*X*) is close to its value in the absence of inhibitor, i.e., $1/(1 + K'_2)$. The conversion of *X* to *W* occurs at a frequency $k_{on}I$ (or $k_{off}I/K'_i$), and the fraction of *W* which recombines is $k_{AP}/(k_{AP} + k_{off})$. Thus, the approximate expression for k_{slow} is

$$k_{slow} \approx \frac{k_{AP}}{1 + K'_2}\left[1 + \frac{Ik_{off}}{K'_i(k_{AP} + k_{off})}\right] = k_{PB}\left(1 + \frac{I}{K'_i}\frac{k_{off}}{k_{AP} + k_{off}}\right) \quad (25)$$

The quantities which are featured in the right-most expression are readily obtained experimentally: k_{BP} is the recombination rate in the absence of inhibitor, and $k_{off}/(k_{AP} + k_{off})$ is the slope of the plot of the fraction of the slow phase versus the inhibited fraction (see eq 23). This expression agrees within better than 1% with the results computed from eq 16, except for the values for terbutryn (due to its large k_{off}) where the discrepancy at large *I* values is about 5%.

We can introduce the direct recombination route from $P^+Q_AQ_B^-$ (with rate constant k_{dir}) in the above scheme. This amounts to adding a term $-k_{dir}K'_2/(1 + K'_2)$ to the expression of γ. Modified expressions for eqs 19 and 20 are easily obtained and can be used to study the dependence of k_{slow} on *I* under such conditions. This shows that eq 25 is still a good approximation, provided k_{dir} is subtracted from the experimental value obtained for k_{slow}.

(5) Kinetics of Inhibitor Displacement. We are now interested in the relaxation of the equilibria following the flash-induced formation of PQ_A^-I in the presence of an electron donor to P^+. The reaction scheme of the preceding section is still valid, if we omit the recombination reaction. The kinetic equation is

$$\frac{dW}{dt} = -k_{off}W + k_{on}IX = \frac{k_{on}IK_q}{1 + K_q + K_2} - W\left(k_{off} + \frac{k_{on}IK_q}{1 + K_q + K_2}\right) \quad (26)$$

The solution is an exponential with the rate constant

$$k_{dis} = k_{off} + \frac{k_{on}IK_q}{1 + K_q + K_2} = k_{off}\left[1 + \frac{I}{K'_i(1 + K'_2)}\right] \quad (27)$$

The initial and final amounts of Q_A^- are given by eqs 4 and 6, respectively. A plot of k_{dis} versus *I* gives a straight line with the intercept k_{off} and the slope $k_{off}/K'_i(1 + K'_2)$.

(6) Effect of Q_A^-. In the above, we ignored the possibility of an influence of the redox state of Q_A on the dissociation constants at the Q_B site (a possible influence of the redox state of P was ignored as well). If this possibility is taken into account, one has to consider different values for K_i and K_q when Q_A is oxidized or reduced, which may be noted, following Wraight, with a superscript D (dark) or L (light), respectively. Thus, the equations of sections 1 and 3−5 involve K_q^L and K_i^L (or $K'_i{}^L$), whereas section 2 involves K_q^D and K_i^D (or $K'_i{}^D$).

The data presented here do not allow the separate measurements of K_q and K_i but of the apparent dissociation constant K'_i, which depends on K_q via eq 5. Therefore, the finding that $K'_i{}^D$ is less than $K'_i{}^L$ may reflect an influence of Q_A^- primarily on K_i (i.e., $K_i^D < K_i^L$) or primarily on K_q (i.e., $K_q^D > K_q^L$) or any combination of both effects. It is noteworthy that if the effect is entirely due to a modified affinity for ubiquinone (i.e., $K_q^D > K_q^L$ and $K_i^D \approx K_i^L$), the release rate of the inhibitor should be the same ($k_{off}^D \approx k_{off}^L$), whereas the apparent rate constant for inhibitor binding ($k'_{on} = k_{off}/K'_i$) should be larger in the even (or D) state than in the odd (or L) state.

REFERENCES

1. Crofts, A. R., and Wraight, C. A. (1983) *Biochim. Biophys. Acta 726*, 149−185.
2. Takamiya, K., and Dutton, P. L. (1979) *Biochim. Biophys. Acta 546*, 1−16.
3. Sled', V. D., Shinkarev, V. P., Verkhovsky, M. I., Grishanova, N. P., and Rubin, A. B. (1985) *Biol. Membr. 2*, 575−587.
4. Stein, R. R., Castellvi, A. L., Bogacz, J. P., and Wraight, C. A. (1984) *J. Cell. Biochem. 24*, 243−259.
5. Stowell, M. H. B., McPhillips, T. M., Rees, D. C., Soltis, S. M., Abresch, E., and Feher, G. (1997) *Science 276*, 812−816.
6. Lancaster, C. R. D. (1998) *Biochim. Biophys. Acta 1365*, 143−150.
7. Okamura, M. Y., and Feher, G. (1995) in *Anoxygenic Photosynthetic Bacteria* (Blankenship, R. E., Madigan, M. T., and Bauer, C. E., Eds.) pp 577−594, Kluwer Academic Publishers, Dordrecht, The Netherlands.
8. Wraight, C. A. (1981) *Isr. J. Chem. 21*, 348−354.
9. Velthuys, B. R. (1982) in *Function of quinones in energy conserving systems* (Trumpower, B. L., Ed.) pp 401−408, Academic Press, New York.
10. Lavergne, J. (1982) *Biochim. Biophys. Acta 682*, 345−353.
11. Diner, B. A., Schenck, C. C., and De Vitry, C. (1984) *Biochim. Biophys. Acta 766*, 9−20.
12. Lavergne, J., and Joliot, P. (1996) *Photosynth. Res. 48*, 127−138.
13. Verméglio, A., Martinet, T., and Clayton, R. K. (1980) *Proc. Natl. Acad. Sci. U.S.A. 77*, 1809−1813.
14. Jenney, F. E., and Daldal, F. (1993) *EMBO J. 12*, 1283−1292.
15. Rott, M. A., Witthuhn, V. C., Schilke, B. A., Soranno, M., Abdulfatah, A., and Donohue, T. J. (1993) *J. Bacteriol. 175*, 358−366.
16. Lavergne, J., Matthews, C., and Ginet, N. (1999) *Biochemistry 38*, 4542−4552.
17. Joliot, P., Béal, D., and Frilley, B. (1980) *J. Chim. Phys. 77*, 209−216.
18. Joliot, P., and Joliot, A. (1984) *Biochim. Biophys. Acta 765*, 210−218.
19. Vermeglio, A., and Clayton, R. K. (1977) *Biochim. Biophys. Acta 461*, 159−165.
20. Verméglio, A. (1982) in *Function of quinones in energy conserving systems* (Trumpower, B. L., Ed.) pp 169−180, Academic Press, New York.
21. Tiede, D. M., Utschig, L., Hanson, D. K., and Gallo, D. M. (1998) *Photosynth. Res. 55*, 267−273.
22. Takahashi, E., and Wraight, C. A. (1990) *Biochim. Biophys. Acta 1020*, 107−111.

23. Labahn, A., Paddock, M. L., McPherson, P. H., Okamura, M. Y., and Feher, G. (1994) *J. Phys. Chem. 98*, 3417−3423.
24. Labahn, A., Bruce, J. M., Okamura, M. Y., and Feher, G. (1995) *Chem. Phys. 197*, 355−366.
25. Allen, J. P., Williams, J. C., Graige, M. S., Paddock, M. L., Labahn, A., Feher, G., and Okamura, M. Y. (1998) *Photosynth. Res. 55*, 227−233.
26. Kleinfeld, D., Abresch, E. C., Okamura, M. Y., and Feher, G. (1984) *Biochim. Biophys. Acta 765*, 406−409.
27. Lancaster, C. R. D., and Michel, H. (1999) *J. Mol. Biol. 286*, 883−898.
28. Allen, J. P., Lous, E. J., Feher, G., Chirino, A., Komiya, H., and Rees, D. C. (1990) in *Current Research in Photosynthesis* (Baltscheffsky, M., Ed.) pp 61−64, Kluwer Academic Publishers, Dordrecht, The Netherlands.
29. Lancaster, C. R. D., Michel, H., Honig, B., and Gunner, M. R. (1996) *Biophys. J. 70* (6), 2469−2492.
30. Alexov, E., Miksovska, J., Schiffer, M., Hanson, D. K., and Gunner, M. R. (2000) *Biochemistry 39*, 5940−5952.
31. Miksovska, J., Schiffer, M., Hanson, D. K., and Sebban, P. (1999) *Proc. Natl. Acad. Sci. U.S.A. 96*, 14348−14353.
32. Knaff, D. B. (1975) *Biochim. Biophys. Acta 376*, 583−587.
33. Krieger-Liszkay, A., and Rutherford, A. W. (1998) *Biochemistry 37*, 17339−17344.
34. Miksovska, J., Maroti, P., Tandori, J., Schiffer, M., Hanson, D. K., and Sebban, P. (1996) *Biochemistry 35*, 15411−15417.
35. Grafton, A. K., and Wheeler, R. A. (1999) *J. Phys. Chem. B 103*, 5380−5387.
36. Mulkidjanian, A. (1999) *FEBS Lett. 463*, 199−204.
37. Baciou, L., and Sebban, P. (1995) *Photochem. Photobiol. 62*, 271−278.
38. Pelusa, A., Di Donato, M., and Saracino, G. A. A. (2000) *J. Chem. Phys. 113*, 3212−3218.
39. Ginet, N., and Lavergne, J. (2000) *Biochemistry 39*, 16252−16262.

BI001686A